Schiff base receives a proton from the cytoplasm, and Asp^{85} finally releases its proton to the extracellular space. If Asp^{85} is missing, the HR mechanism comes into action also for BR when chloride is present. The third mode of action is active in both molecules when both the fixed charge of Asp^{85} and the movable charge of chloride are missing. After dipole flipping, the Schiff base in its high-energy state releases the proton to the cytoplasmic surface as the only choice to relax thermodynamically. As a result, a proton is picked up from the extracellular space after several intermediary steps and proton translocation is observed with inversed vectoriality.

In summary, the high-resolution structure of HR presented here provides a key to understand this case of active transport in both directions by and on the same molecule. Future crystallographic studies on photointermediates of HR should track chloride on its course through this integral membrane protein after photoexcitation.

References and Notes

1. P. D. Boyer, *Annu. Rev. Biochem.* **66**, 717 (1997).
2. D. Oesterhelt, *Curr. Opin. Struct. Biol.* **8**, 489 (1998).
3. B. P. Rosen *et al.*, *Biochim. Biophys. Acta* **1018**, 203 (1990).
4. M. Ikeda and D. Oesterhelt, *Biochemistry* **29**, 2065 (1990).
5. D. Oesterhelt, *Isr. J. Chem.* **35**, 475 (1995).
6. B. Schobert and J. K. Lanyi, *J. Biol. Chem.* **257**, 10306 (1982).
7. W. Havelka *et al.*, *J. Mol. Biol.* **247**, 726 (1995).
8. T. Arlt *et al.*, *Chem. Phys. Lett.* **241**, 559 (1995).
9. E. Bamberg, J. Tittor, D. Oesterhelt, *Proc. Natl. Acad. Sci. U.S.A.* **90**, 639 (1993).
10. J. Sasaki *et al.*, *Science* **269**, 73 (1995).
11. J. Tittor *et al.*, *J. Mol. Biol.* **271**, 405 (1997).
12. HR (mature form: 253 amino acids, molecular mass = 26,962 daltons) was homologously overexpressed in the *H. salinarum* strain D2 as described (*32*). DNA sequencing of the *hop* gene showed a single point mutation, $Val^{229} \rightarrow$ Ala, which is located in a functionally unimportant region of the FG loop. Isolation and purification of the membrane fraction containing HR were performed according to (*33*). HR, solubilized in 5% (w/v) cholate, 4 M KCl, and 50 mM tris-HCl (pH 7.2), was applied to a phenyl-sepharose CL-4B column (Pharmacia), washed with 0.4% (w/v) cholate buffer, and eluted by changing to 1% (w/v) β-octyl-glucoside in the same buffer. HR was concentrated on 50-kD cutoff membrane filters (Amicon) and batchwise incorporated into a cubic lipidic phase as previously described (*14*). Optimal crystallization conditions were found at a final composition of 58 to 62% (w/w) 1-monooleoyl-*rac*-glycerol, 4 M KCl, HR (3.3 to 4.0 mg/ml), and 50 mM tris-HCl (pH 6.5 to 7.4) (22°C, dark). Small crystals of HR formed within 2 weeks and attained final sizes of 0.1 mm by 0.1 mm by 0.02 mm.
13. L.-O. Essen *et al.*, *Proc. Natl. Acad. Sci. U.S.A.* **95**, 11673 (1998).
14. E. Landau and J. P. Rosenbusch, *Proc. Natl. Acad. Sci. U.S.A.* **93**, 14532 (1996).
15. J. Barauskas *et al.*, *Chem. Phys. Lipids* **97**, 167 (1999).
16. H. Luecke *et al.*, *J. Mol. Biol.* **291**, 899 (1999).
17. H. Belrhali *et al.*, *Struct. Folding Des.* **7**, 909 (1999).
18. I. Pascher *et al.*, *Biochem. Biophys. Acta* **1113**, 339 (1992).
19. K. Ihara *et al.*, *J. Mol. Biol.* **285**, 163 (1999).
20. J. Otomo, *Biophys. Chem.* **56**, 137 (1995).
21. D. Okuno *et al.*, *Biochemistry* **38**, 5422 (1999).
22. T. Alshuth *et al.*, *FEBS Lett.* **179**, 55 (1985).
23. M. Rüdiger and D. Oesterhelt, *EMBO J.* **16**, 3813 (1997).
24. T. J. Walter and M. S. Braiman, *Biochemistry* **33**, 1724 (1994).
25. B. Schobert *et al.*, *J. Biol. Chem.* **261**, 2690 (1986).
26. M. Rudiger *et al.*, *EMBO J.* **14**, 1599 (1995).
27. M. S. Braiman, T. J. Walter, D. M. Briercheck, *Biochemistry* **33**, 1629 (1994).
28. A. Corcelli *et al.*, *Biochim. Biophys. Acta* **1281**, 173 (1996).
29. K. Edman *et al.*, *Nature* **401**, 6755 (1999).
30. I. V. Kalaidzidis *et al.*, *FEBS Lett.* **427**, 59 (1998).
31. Y. S. Chon *et al.*, *Biochemistry* **38**, 9449 (1999).
32. J. A. W. Heymann, W. A. Havelka, D. Oesterhelt, *Mol. Microbiol.* **7**, 623 (1993).
33. A. Duschl, M. A. McCloskey, J. K. Lanyi, *J. Biol. Chem.* **263**, 17016 (1988).
34. Single-letter abbreviations for the amino acid residues are as follows: A, Ala; C, Cys; D, Asp; E, Glu; F, Phe; G, Gly; H, His; I, Ile; K, Lys; L, Leu; M, Met; N, Asn; P, Pro; Q, Gln; R, Arg; S, Ser; T, Thr; V, Val; W, Trp; and Y, Tyr.
35. P. J. Kraulis, *J. Appl. Crystallogr.* **24**, 946 (1991).
36. V. Reat *et al.*, *Proc. Natl. Acad. Sci. U.S.A.* **95**, 4970 (1998).
37. M. Colella *et al.*, *Biochim. Biophys. Acta* **1370**, 273 (1998).
38. M. Kolbe, H. Besir, L.-O. Essen, D. Oesterhelt, data not shown.
39. D. Bashford and K. Gerwert, *J. Mol. Biol.* **224**, 473 (1992).
40. U. Haupts *et al.*, *Biochemistry* **36**, 2 (1997).
41. A. G. W. Leslie, in *Joint CCP4 and ESF-EACMB Newsletter on Protein Crystallography No. 26* (Daresbury Laboratory, Warrington, UK, 1992), pp. 44–51.
42. CCP4, *Acta Crystallogr. D* **50**, 760 (1994).
43. A. T. Brünger *et al.*, *Acta Crystallogr. D* **54**, 905 (1998).
44. G. Varo *et al.*, *Biophys. J.* **68**, 2062 (1995).
45. R. A. Laskowski *et al.*, *J. Appl. Crystallogr.* **26**, 283 (1993).
46. A. Nicholls, K. A. Sharp, B. Honig, *Proteins* **11**, 281 (1991).
47. M. R. Gunner, unpublished data.
48. P. Tavan, K. Schulten, D. Oesterhelt, *Biophys. J.* **47**, 415 (1985).
49. P. Beroza and D. A. Case, *J. Phys. Chem.* **100**, 20156 (1996).
50. The authors are very grateful for support by H. Bartunik at synchrotron beamline BW6, Max-Planck groups for structural molecular biology, Hamburg, W. Burmeister at ID14-3, European Synchrotron Radiation Facility Grenoble, and J. Tittor for discussion and DNA sequencing. This work was supported by EU grant BIO4-CT98-0415, Sonderfarschungsbereich 533 (Deutsche Forschungsgemeinschaft), and the Fonds der Chemischen Industrie. Coordinates and structure factors are available from the Protein Data Bank (accession number 1E12).

3 March 2000; accepted 1 May 2000

REPORTS

Anomalous Polarization Profiles in Sunspots: Possible Origin of Umbral Flashes

H. Socas-Navarro,[1] J. Trujillo Bueno,[1,2] B. Ruiz Cobo[1,3]

We present time-series spectropolarimetric observations of sunspots in the Ca II infrared triplet lines, which show a periodic occurrence of anomalous, asymmetric, circular polarization profiles in the umbral chromosphere. The profiles may be caused by the periodic development of an unresolved atmospheric component in a downward flowing magnetized environment. This active component with upward directed velocities as high as 10 kilometers per second is connected to the umbral flash (UF) phenomenon. We can explain the observations with a semiempirical model of the chromospheric oscillation and of the sunspot magnetized atmospheric plasma during a UF event.

Sunspots provide us with a unique example of a magnetically structured plasma through the study of which we may hope to understand a variety of radiation magnetohydrodynamic phenomena. Of particular interest in this respect are the sunspot chromospheric oscillations and the UFs (*1–4*). Presently considered as one of the most dramatic dynamic phenomena that take place in sunspots (*5*), UFs have traditionally been associated with the release of large amounts of thermal energy in the chromosphere (*6*). The most relevant known facts about UFs may be summarized as follows (*1*, *2*): UFs consist of the sudden core brightening of the intensity profiles in the chromospheric Ca II lines observed in the umbra of some sunspots. The lines rapidly develop a blueshifted emission core, which reaches a maximum intensity and later disappears, the line profile returning to its quiet preflash shape. The horizontal spatial extent of UFs varies between about 2000 and 3500 km. The rise time of the flash, from the beginning to the phase of maximum intensity, is about 20 to 30 s. The decay back to the quiet state is slower, about 1 min. UFs

[1]Instituto de Astrofísica de Canarias, E-38200 La Laguna, Tenerife, Spain. [2]Consejo Superior de Investigaciones Científicas, Spain. [3]Departamento de Astrofísica, Universidad de La Laguna, Tenerife, Spain.

tend to occur at regular time intervals, repeating themselves periodically every 2.5 to 3 min. Sometimes, however, they only show up sporadically. UFs are connected with the chromospheric umbral oscillation. This oscillation is detected as periodic variations in some parameters measured in the chromospheric lines, such as the line minimum positions and line core intensities. When a sunspot exhibits periodic UFs, the UFs occur with the same periodicity as the umbral oscillation. Not every sunspot exhibits flashes, but so far it has not been possible to find a distinctive common feature shared by all of the sunspots with UFs. A statistical analysis of a large number of sunspot groups (*7*) has revealed that UFs show up in sunspots of all sizes, morphologies, and magnetic field strengths.

We observed time series of the intensity (*I*) and circular polarization (*V*) Stokes profiles (*8*) emergent from two sunspots near the solar disk center using the German Gregory Coudé Telescope (*9*), at the Spanish Observatorio del Teide of the Instituto de Astrofísica de Canarias (*10*). These were the sunspots cataloged as NOAA 8338 and NOAA 8340 (hereafter referred to as S-A and S-B, respectively). S-A is a round, fairly symmetric sunspot, whereas S-B shows an asymmetric geometry with two umbrae separated by a thin region of light. Each time series consists of a set of images taken every 36 s over about an hour, with an exposure time of 10 s. The photospheric Fe I line at 8497 Å and the chromospheric Ca II lines at 8498 and 8542 Å were simultaneously recorded in each image. In the data analysis process, we carried out a second-order flat-field correction (*11*) to achieve a polarimetric accuracy of 10^{-3}. By this figure, we mean that the noise on the Stokes *V* profiles is about 10^{-3} times the quiet sun continuum intensity at 5000 Å.

The data obtained show that the Stokes *I* profiles emergent from S-A always remain in a quiet state and do not exhibit UFs (Fig. 1, A and C). The oscillations in the line core intensity and position exhibit a clear period of about 2.5 min. In spite of this "quietness," examination of the polarization signal emergent from this sunspot shows that the "normal," antisymmetric shape of the Stokes *V* profiles (Fig. 1B) of the chromospheric Ca II lines periodically changes to an anomalous, strongly asymmetric shape (Fig. 1D), returning to the their normal state (Fig. 1B) after a period of 2.5 min. The photospheric Fe I line at 8497 Å does not exhibit this behavior and maintains a fairly antisymmetric shape at all times. S-B, on the other hand, shows very active behavior in Stokes *I*, with sporadic UFs visible from time to time in the cores of the Ca II lines (see Fig. 1E). The circular polarization profiles of the chromospheric lines in S-B exhibit a particularly striking asymmetry during the flash events (see Fig. 1F).

In principle, three mechanisms could produce asymmetries on the observed line profiles. These mechanisms are the atomic orientation (*12*), the effects of velocity and magnetic field gradients along the line of sight in a single-component atmosphere, and the presence of different atmospheric structures within the resolution element of the observations. Numerical simulations of the radiative transfer accounting for the Zeeman effect, and considering departures of the local thermodynamical equilibrium (LTE) (i.e., including non-LTE effects), allowed us to discard the atomic orientation scenario and also that based on the presence of velocity and magnetic field gradients in a single-component atmosphere. Moreover, a detailed analysis of our observations confirmed that the anomalous Stokes *V* profiles can be understood if we consider two unresolved atmospheric components. The first component produces normal profiles, such as those observed during the quiet phase of the oscillation. The second component, on the other hand, produces profiles with a blueshifted emission feature in the line cores (i.e., with core reversals). Therefore, this second unresolved component produced flashlike profiles in S-A, but its filling factor (i.e., the percentage of the resolution element covered by this component) was too small and the UFs were not directly visible in the observations of the intensity profiles. These results suggest that the answer to the question of why only some sunspots exhibit UFs may be that they are actually present in all of them, being visible only when the filling factor of this second component is large enough.

A non-LTE inversion method of polarization signals induced by the Zeeman effect (*13*, *14*) was applied to the observed data to recover the depth stratification of the thermodynamic variables (temperature, pressure, line-of-sight velocity, and microturbulence) and the magnetic field vector in the solar atmosphere. In this manner, we derived a time-dependent semiempirical model umbra of S-A over a whole oscillation cycle. We find that all the profiles can be reproduced with the same scenario, consisting of two unresolved atmospheric components (Fig. 2). The first component (solid lines) has downward velocities, and its temperature, density, and magnetic field vector are typical of a mean model of a sunspot umbra. The second component (dotted lines) is similar to the first, except that its velocities are directed upward, reaching values as high as 10 km s^{-1}. The optical depth scale of the second component, however, is shifted in the chromosphere with respect to that of the first component. The same scenario is capable of reproducing the profiles throughout the oscillation cycle (and even the UF profiles) by changing the filling

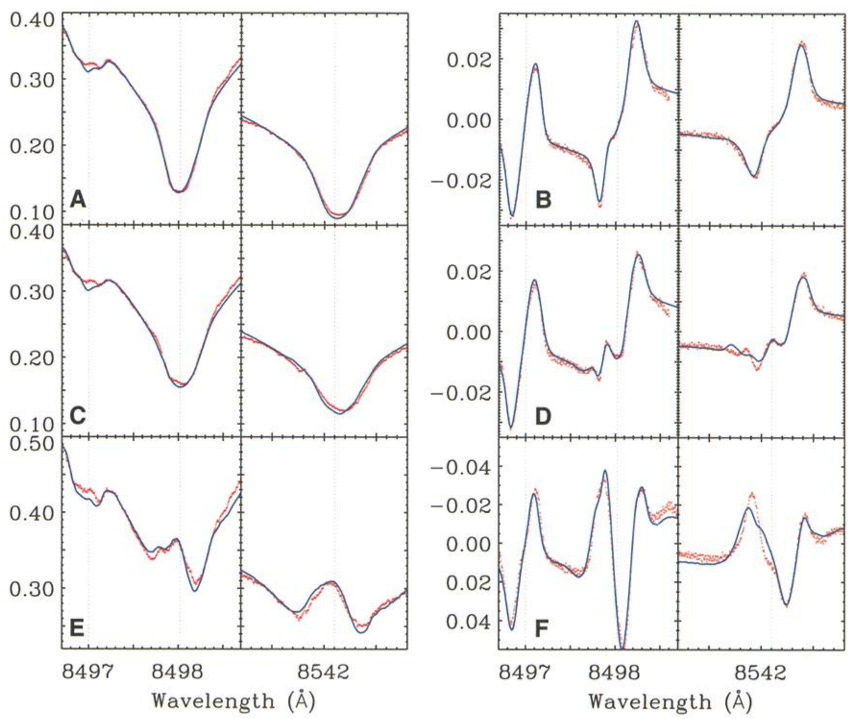

Fig. 1. Stokes *I* (left) and *V* (right) profiles observed (red dots) in a sunspot umbra at different times and the corresponding fits provided by our non-LTE inversion method (blue line). The profiles are normalized to the intensity of the quiet sun continuum at 500 nm. (**A**) and (**B**) show the normal profiles, with the characteristic antisymmetric shape of Stokes *V*, observed during the quiet phase. (**C**) and (**D**) show the normal Stokes *I* and anomalous Stokes *V* profiles that periodically occur in S-A. (**E**) and (**F**) show the UF profiles observed in S-B. The vertical dotted lines mark the central rest wavelength of the three lines.

factor of the second component as time goes by. In particular, the profiles shown in Fig. 1 yield values for the filling factor of 4% (Fig. 1, A and B) and 12% (Fig. 1, C and D).

Our semiempirical, time-dependent, two-component model suggests two possible physical scenarios for the UF phenomenon, depending on whether or not we adopt the hypothesis that the thermal structure of both unresolved atmospheric components is the same at equal geometric heights. The first scenario is characterized by periodic mass ejections from the underlying photosphere. Because the photosphere is much denser (by a factor of about 10^4) than the chromosphere, a very small fraction of photospheric material would be enough to increase the chromospheric opacity and lead to the above-mentioned shift of the optical depth scales (Fig. 2). In this physical scenario, the emission reversal observed in the UF would not be due to a sudden heating of the material but rather to a shift of the line formation region to higher (and therefore hotter) layers. The driving source for the photospheric ejections would be the umbral photospheric 3-min oscillation [although the dominant oscillation period in the photosphere is 5 min, many authors have reported a weak umbral oscillation (*4*, *5*) just above the noise level with a period of between 2.5 and 3 min]. This picture is supported by the strong correlation found between the 3-min oscillation in the photosphere and that in the chromosphere (*15*).

This model of the sunspot atmospheric plasma during the oscillation cycle allows us to estimate the time-dependent mass upflows and downflows involved in the process. This estimate indicates that there is a net mass downflow during the quiet phase of the oscillation and a net upflow during the UF event. However, when the total oscillation cycle is considered, it turns out that the net time-integrated mass upflows and downflows are very similar, even though mass conservation was never imposed as a constraint in the derivation of the model. This net mass conservation over the whole oscillation cycle is of interest in relation to the mass and energy balance of the outermost atmospheric layers. In fact, in review papers on the subject, it has been argued that there exists a net upflow of the chromospheric material in the oscillation (*6*), and, more recently, it has been pointed out (*16*) that for sunspots we do not know if the umbral chromospheres show a net upflow or downflow because, at high resolution, the observations are compromised by the oscillatory dynamics.

Alternatively, if we do not assume equality of the kinetic temperatures for the two unresolved components at equal geometric heights, our models may then be interpreted in terms of waves propagating upward in a downflowing magnetized environment and eventually leading to shocks. This physical scenario is related to the most commonly accepted view (*5*) that UFs are caused by the nonlinear steepening of the 3-min umbral oscillations in the chromosphere. However, we should emphasize that our observations cannot be simply explained by wave propagation and shock-wave formation in a single-component umbral atmosphere. Our suggested second physical scenario is wave propagation in a three-dimensional magnetized medium with downflowing velocities. In this scenario, the active component would be that associated with shock-wave formation, which would take place at the instant at which the filling factor is the largest.

The downward directed mass flows in the sunspot umbra might be related to the inverse Evershed flow (*17*) and/or to the so-called "redshift phenomenon" (*18*) observed in lines formed in the higher atmosphere. The investigation of the interesting issues of whether and how the photospheric 3-min oscillations could be triggering the mass ejections or whether the UF phenomenon is simply the natural outcome of propagating shock waves in a downflowing magnetized environment urgently demands detailed three-dimensional radiation magnetohydrodynamic simulations of the sunspot chromospheres.

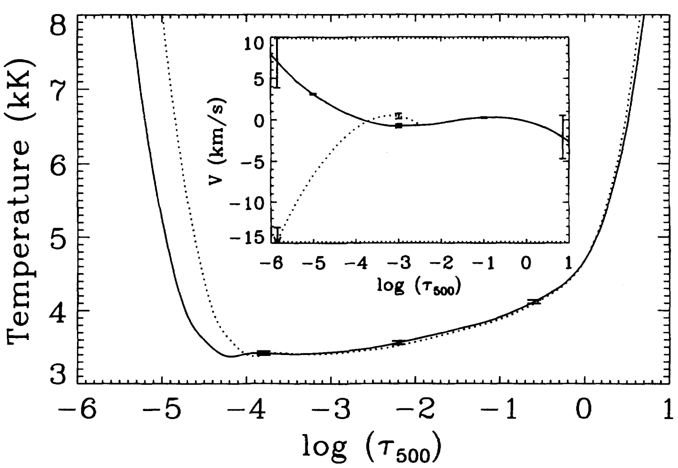

Fig. 2. Temperature and velocity (V, **inset**) stratification in our two-component model umbra during the occurrence of anomalous Stokes *V* profiles. The symbol τ_{500} stands for the continuum optical depth at 500 nm. Positive velocities are directed downward (i.e., toward the stellar interior). The solid lines refer to the first atmospheric component, whereas the dotted lines indicate the second atmospheric component. The vertical segments indicate the error bars.

References and Notes

1. J. M. Beckers and P. E. Tallant, *Sol. Phys.* **7**, 351 (1969).
2. A. Wittmann, *Sol. Phys.* **7**, 366 (1969).
3. F. Kneer, W. Mattig, M. von Uexküll, *Astrophys. J.* **102**, 147 (1984).
4. J. H. Thomas, L. E. Cram, A. H. Nye, *Astron. Astrophys.* **285**, 368 (1984).
5. B. W. Lites, in *Sunspots: Theory and Observations*, vol. 375 of *NATO ASI Series*, J. H. Thomas and N. O. Weiss, Eds. (Kluwer Academic, Dordrecht, Netherlands, 1992), pp. 261–302.
6. R. L. Moore, *Space Sci. Rev.* **28**, 387 (1981).
7. I. P. Turova, *Sol. Phys.* **91**, 51 (1984).
8. It is common in astrophysics to represent the spectral properties of the intensity and polarization state of the light in terms of a frequency-dependent Stokes vector. The components of this vector, denoted as *I*, *Q*, *U*, and *V*, describe the intensity (*I*), linear polarization along two reference axes (*Q* and *U*), and circular polarization (*V*) (*19*).
9. E. H. Schröter, D. Soltau, E. Wiehr, *Vistas Astron.* **28**, 519 (1985).
10. The observations were carried out on 22 September 1998. On this particular day of the year, the declination of the sun was very close to 0°, which implies that the contamination introduced into the data by instrumental polarization is negligible (*20*). The polarization analyzer used was a standard circular analyzer (*21*), consisting of a $\lambda/4$ plate and a calcite beam splitter placed after the entrance slit of the spectrograph. The instrumental cross talk between circular and linear polarization was minimized by carefully aligning the polarimeter in the laboratory with a He-Ne laser.
11. J. Sánchez Almeida and V. Martínez Pillet, *Astrophys. J.* **424**, 1014 (1994).
12. J. Trujillo Bueno *et al.*, in *The Magnetic and Velocity Fields of Solar Active Regions*, vol. 46 of *Astronomical Society of the Pacific Conference Series*, H. Zirin, A Gouxiang, H. Wang, Eds. (Astronomical Society of the Pacific, San Francisco, CA, 1993), pp. 526–529.
13. H. Socas-Navarro, B. Ruiz Cobo, J. Trujillo Bueno, *Astrophys. J.* **507**, 470 (1998).
14. H. Socas-Navarro, J. Trujillo Bueno, B. Ruiz Cobo, *Astrophys. J.* **530**, 977 (2000).
15. B. W. Lites and J. H. Thomas, *Astrophys. J.* **294**, 682 (1985).
16. B. W. Lites, in *Chromospheric Dynamics, Proceedings of a Mini-Workshop Held at the Institute of Theoretical Astrophysics, University of Oslo, Norway*, M. Carlsson, Ed. (Institute of Theoretical Astrophysics, Oslo, Norway, 1994), pp. 1–23.
17. J. H. Thomas and N. O. Weiss, in *Sunspots: Theory and Observations*, vol. 375 of *NATO ASI Series*, J. H. Thomas and N. O. Weiss, Eds. (Kluwer Academic, Dordrecht, Netherlands, 1992), pp. 3–59.
18. P. Maltby, in *1st Advances in Solar Physics Euroconference. Advances in Physics of Sunspots*, vol. 118 of *Astronomical Society of the Pacific Conference Series*, B. Schmieder, J. C. del Toro Iniesta, M. Vazquez, Eds. (Astronomical Society of the Pacific, San Francisco, CA, 1997), pp. 91–110.
19. S. Chandrasekhar, *Radiative Transfer* (Dover, New York, 1960).
20. J. Sánchez Almeida *et al.*, *Sol. Phys.* **134**, 1 (1991).
21. M. Semel, *Astron. Astrophys.* **91**, 369 (1980).

22. We thank J. Sánchez Almeida for his advice during the observations and the data analysis, R. Rutten for valuable discussions and suggestions, and T. Mahoney for his careful reading of the report. Partial financial support from the Spanish Dirección General de Enseñanza Superior through project PB 95-0028-C is also acknowledged. This research is part of the ongoing European Commission–Training and Mobility of Researchers European Solar Magnetometry Network.

18 February 2000; accepted 11 April 2000